5	Synthetic	Glecaprevir	-1.80	
6		Simeprevir	-6.04	
7		Indinavir	0.29	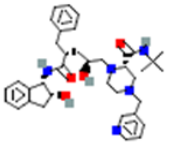

Pseudopterosin A exhibits h-bond interactions in GLU 166, HIS 163, CYS 145, GLY 143, LEU 141, SER 144, and ASN 142 during molecular interaction analysis from which GLU 166, GLN 192, and THR 190 residues were found to be stable after the MD simulation. Here the GLU 166 residue remains stable even after the 100 ns MD simulation (Figure 1). In the MD trajectory analysis of the 6LU7-psuedoteridopsin A complex, the mean RMSD values in the backbone were 0.574 nm, and the RMSD values varied between 0.9788 nm and 0.0004 nm. The graph shows an observable deviation up to 63 ns and an equilibrated state from 63 ns to 95 ns with an average of 0.870 nm. The RMSF implies that the regions from residue index 274-279 show fluctuation between 0.82 nm to 1.085 nm, residue index 195-197 show fluctuation between 0.796 nm to 0.925 nm, and residue index 72-78 show fluctuation between 0.799 nm to 0.817 nm. The RoG of the complex fluctuates between 2.37 nm to 2.15 nm with an average of 2.23 nm. The 6LU7-psuedoteridopsin A complex has an average SASA value of 151.2239 nm^2 and ranges from 161.392 nm^2 to 141.617 nm^2 (Figure 2).

Figure 1. Molecular interaction between psuedoteridopsin A and SARS-CoV-2 main protease (6LU7). (A) Interaction of psuedoteridopsin A-6LU7 complex after molecular docking; (B) Binding pose of docked complex, psuedoteridopsin A-6LU7 in hydrophobic surface view; (C) H-bond residues of docked complex, psuedoteridopsin A-6LU7; (D) Interaction of psuedoteridopsin A-6LU7 complex after MD simulation; (E) MD result of psuedoteridopsin A-6LU7 complex in hydrophobic surface view; (F) H-bond residues of psuedoteridopsin A-6LU7 complex after MD simulation.

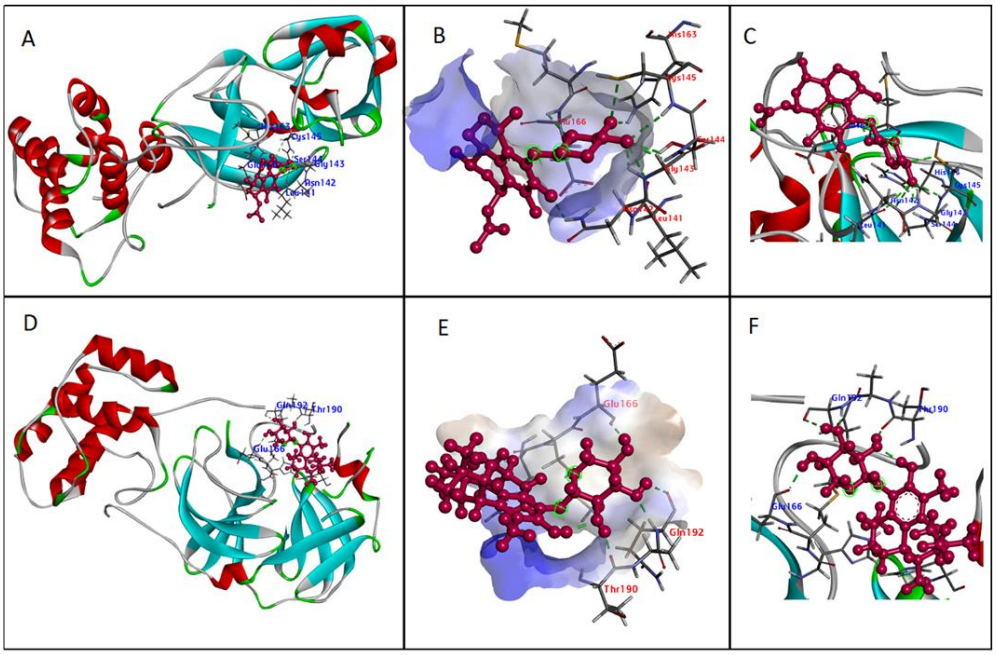

Figure 2. Trajectory plots of psuedoteridopsin A-6LU7 MD simulation. (A) RMSD plot of psuedoteridopsin A-6LU7 MD simulation; (B) RMSF plot psuedoteridopsin A-6LU7 MD simulation; (C) Radius of gyration plot of psuedoteridopsin A-6LU7 MD simulation; (D) H-bond distribution plot of psuedoteridopsin A-6LU7 MD simulation.

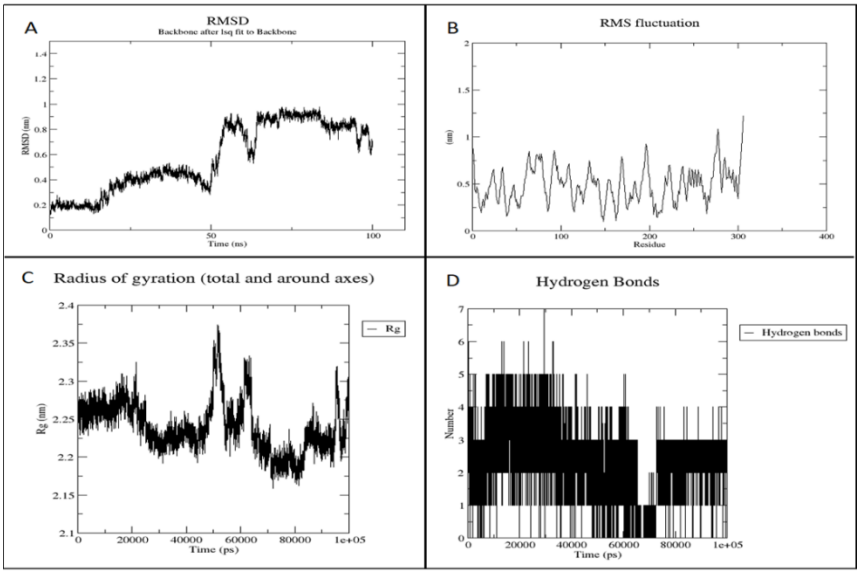

Simeprevir is an oral drug that acts directly to inhibit hepatitis C virus protease (HCV NS3/4A) and is used in HCV infection in adults. As they are macrocyclic compounds, the structure itself helps to enhance the affinity and selectivity for speedy association and slow dissociation to the receptor molecule via non-covalent binding. This antiviral drug is highly efficacious and safe, with fewer side effects. The molecular interaction analysis exhibits h-bond interactions in LEU 141, SER 144, CYS 145, GLU 166, and molecular dynamic simulation exhibits h-bond interactions in CYS 145, GLU 166, SER 144, GLY 143, and HIS 41 residues. The residues CYS 145, GLU 166, and SER 144 present in molecular docking remain stable after MD simulation (Figure 3). Here most of the residues involve in receptor-ligand binding are stable [19].

Figure 3. Molecular interaction between Simeprevir and SARS-CoV-2 main protease (6LU7). (A) Interaction of Simeprevir-6LU7 complex after molecular docking; (B) Binding pose of docked complex, Simeprevir-6LU7 in hydrophobic surface view; (C) H-bond residues of docked complex, Simeprevir-6LU7; (D) Interaction of Simeprevir-6LU7 complex after MD simulation; (E) MD result of Simeprevir-6LU7 complex in hydrophobic surface view. (F) H-bond residues of Simeprevir-6LU7 complex after MD simulation.

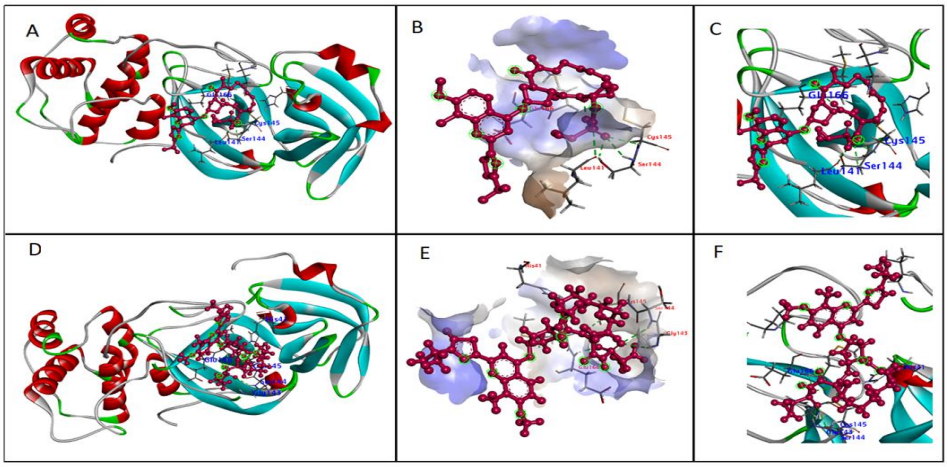

In MD trajectory analysis, the mean RMSD values in the backbone of the 6LU7-Simeprevir complex were 0.211 nm and the RMSD values varied between 0.3675 nm and 0.0005 nm. After the initial deviation, the RMSD value attains equilibrium from 50 ns to 75 ns with an average of 0.180 nm which is so close to the total average, followed by a slight slope in the plot to attain the maximum value of 0.3675 nm [20].

The RMSF of the complex implies that both terminal ends showed higher fluctuations as they are highly dynamic in

nature. The highly fluctuating region is from residue index 46 to 56 with RMSF values ranging from 0194 nm to 0.3 nm. Other residues showing high RMSF values are residues 169, 168, and 191 with values of 0.278 nm, 0.238 nm, and 0.225 nm respectively. The RoG fluctuates between 2.31 nm to 2.19 nm with an average of 2.25 nm. For the 6LU7-psuedoteridopsin The SASA value for the complex has an average value of 152.8134 nm^2 and ranges from 161.319 nm^2 to 144.579 nm^2 (Figure 4).

Figure 4. Trajectory plots of Simeprevir-6LU7 MD simulation. (A) RMSD plot of Simeprevir-6LU7 MD simulation; (B) RMSF plot Simeprevir-6LU7 MD simulation; (C) Radius of Gyration plot of Simeprevir-6LU7 MD simulation; (D) H-bond distribution plot of Simeprevir-6LU7 MD simulation.

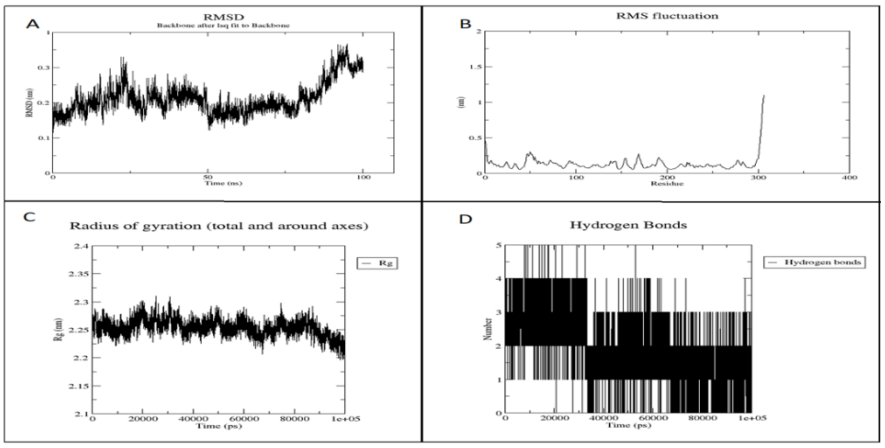

CONCLUSION

The current study is an *in-silico* approach to repurpose the commercially antiviral drugs against SARS-CoV-2. Molecular interaction analysis and further MD validation of a set of 40 drug molecules and the SARS-CoV-2 main protease were performed. The Binding free energy of the top-ranked receptor-ligand complexes was calculated using MMPBSA. In the study, pseudopterosins from marine sources (Caribbean Sea whip-pseudopterogoria elisabethae) shows noticeable interaction with the target molecule. The molecular dynamic simulation and MMPBSA results imply that pseudopterosin A and simeprevir show promising interactions and binding affinity against the receptor. The potentiality of these drug molecules against the virus brings new hope for COVID-19 medications. Further clinical analysis is needed to validate the activity.

Acknowledgments

This research was supported by Accubits Invent Pvt Ltd and supervised by Dr. Nidhin Sreekumar, chief research scientist. We thank all our colleagues who provided insight and expertise that greatly assisted the research. We are immensely grateful to Dr. Suvanish Kumar, Research Scientist of Accubits Invent Pvt Ltd for his assistance with constructive criticism and comments that significantly improved the manuscript. We thank Dr. Jyothi B Nair, Research Scientist of Accubits Invent Pvt Ltd for her comments on an earlier version of the manuscript.

Author contributions

Shahanas Naisam conceived of the presented idea, and designed the work plan and computational framework. Aswin Mohan, Gayathri S S, and Sidharth Selvin performed the data collection and computations. Shahanas Naisam and Dr. Nidhin Sreekumar verified the result. Dr. Nidhin Sreekumar encouraged the investigation and supervised the findings of this work. All authors discussed the results and contributed to the final manuscript.

Conflicts of interest

The authors declare no conflict of interest in publishing the article.

REFERENCES

1. Abraham MJ, et al. GROMACS: High performance molecular simulations through multi level parallelism from laptops to supercomputers. SoftwareX. 2015;1:19-25.

2. Badria FA, et al. Sarcophytolide: A new neuroprotective compound from the soft coral Sarcophyton glaucum. Toxicology. 1998;131:133-143.
3. Barbieri F, et al. Repurposed biguanide drugs in glioblastoma exert antiproliferative effects via the inhibition of intracellular chloride channel 1 activity. Front Oncol. 2019;9:135.
4. Brainerd HD, et al. Methisazone in progressive vaccine. N Engl J Med. 1967;276:620-622.
5. Chrisp P, et al. Foscarnet. Drugs. 1991;41:104-129.
6. Chu CM, et al. Role of lopinavir/ritonavir in the treatment of SARS: initial virological and clinical findings. Thorax. 2004;59:252-256.
7. Correa H, et al. Cytotoxic and antimicrobial activity of pseudopterosins and seco-pseudopterosins isolated from the octocoral pseudopterogorgia elisabethae of San Andrés and Providencia Islands (Southwest Caribbean Sea). Mar Drugs. 2011;9:334-344.
8. Gogineni V, et al. Role of marine natural products in the genesis of antiviral agents. Chem Rev. 2015;115:9655-9706.
9. Guan S, et al. Exploration of binding mechanism of a potential streptococcus pneumoniae neuraminidase inhibitor from herbaceous plants by molecular simulation. Int J Mol Sci. 2020;21:1003.
10. Horwitz JP, et al. The Monomesylates of 1-(2'-Deoxy-β-D-lyxofuranosyl) thymine1, 2. J Org Chem. 1964;29:2076-2078.
11. Hou XM, et al. Marine natural products as potential anti-tubercular agents. Eur J Med Chem. 2019;165:273-292.
12. Ikematsu H, et al. Laninamivir octanoate: A new long acting neuraminidase inhibitor for the treatment of influenza. Expert Rev Anti Infect Ther. 2011;9:851-857.
13. Izquierdo L, et al. Simeprevir for the treatment of hesanderpitis C virus infection. Pharmgenomics Pers Med. 2014;7:241.
14. Katsumura S, et al. Total synthesis of manoalide and seco-manoalide. Tetrahedron letters. 1985;26:5827-5830.
15. Keyaerts E, et al. Antiviral activity of chloroquine against human coronavirus OC43 infection in newborn mice. Antimicrob Agents Chemother. 2009;53:3416-3421.
16. Kushwaha PP, et al. Identification of natural inhibitors against SARS-CoV-2 drugable targets using molecular docking, molecular dynamics simulation, and MM-PBSA approach. Front Cell Infect Microbiol. 2021:728.
17. Lamb YN, et al. Glecaprevir/pibrentasvir: First global approval. Drugs. 2017;77:1797-1804.
18. Laport MS, et al. Marine sponges: Potential sources of new antimicrobial drugs. Curr Pharm Biotechnol. 2009;10:86-105.
19. Liu C, et al. Research and development on therapeutic agents and vaccines for COVID-19 and related human coronavirus diseases. ACS Cent Sci. 2020;6:315-331.
20. Loya S, et al. Mode of inhibition of HIV-1 reverse transcriptase by polyacetylenetriol, a novel inhibitor of RNA and DNA directed DNA polymerases. Biochem J. 2002;362:685-692.